J. Plasma Fusion Res. SERIES, Vol. 4 (2001) 124–130

Controlled Experiment on Two-Dimensional Vortex Dynamics in Electron Plasma

KIWAMOTO Yasuhito*, ITO Kiyokazu[1] and SANPEI Akio[1]
Faculty of Integrated Human Studies, Kyoto UniversitySakyo-ku, Kyoto 606-8501, Japan
[1]*Graduate School of Human and Environmental Studies, Kyoto University, Sakyo-ku 606-8501, Japan*

(Received: 5 December 2000 / Accepted: 27 August 2001)

Abstract

Fundamental processes in 2-dimensional turbulence are studied experimentally in terms of vortex dynamics in an electron plasma on the theoretical basis of the isomorphism between the Euler fluid and the guiding-center electron fluid. The initial distribution of the vorticity is controlled precisely in a wide spectrum of shape and strength by using an array of small electron emitters. By employing imaging diagnostics we examine key elementary processes at work behind the successive appearance of quasi-equilibrium "crystallized" states of decreasing number of discrete vortices. The observation includes dynamics of a single or two discrete vortices interacting each other or with an extended background vortex, and structural deformations of the background vorticity distribution.

Keywords:
electron plasma, vortex, 2-dimensional turbulence

1. Introduction

A set of equations that describe 2-dimensional (2D) motions of guiding centers of electrons transverse to the externally applied homogeneous magnetic filed $B_0\hat{z}$ are isomorphic to those of the 2D Euler fluid of non-charged particles [1]. The relation $\zeta = en_e/\varepsilon_0 B_0 = \omega_p^2/\omega_c$ between the electron density $n_e(x,y)$ and the vorticity $\zeta(x,y) = \zeta\hat{z} = \nabla \times \boldsymbol{v}$ makes the diagnostics of the flow distribution with $\boldsymbol{v} = \boldsymbol{E} \times \boldsymbol{B}_0/B_0^2 = \hat{z} \times \nabla\phi/B_0$ much easier in the electron plasma. Here ω_p and ω_c are the local plasma and cyclotron frequency, respectively. Since the stream function ψ, defined by $\boldsymbol{v} = \hat{z} \times \nabla\psi$, is related to potential distribution simply by $\phi(x,y) = B_0\psi(x,y)$, the electrostatic analyses are directly applicable to the flow dynamics.

The distribution $\phi(x,y)$ is obtained numerically from $n_e(x,y)$ that is determined experimentally in terms of the 2D luminosity distribution $I(x,y)$ on charge-coupled-device (CCD) camera images [2]. This diagnostics includes dumping of all electrons along the magnetic field lines to an Aluminum-coated phosphor screen that also serves to electronically determine the total charge of electrons $-eN$. The linear relationship has been demonstrated between $I(x,y)$ and the line-integrated electron density distribution $N_l(x,y) = \int dz n_e(x,y,z)$ in a wide dynamic range of 1 : 3000 with a high sensitivity of 1 count per 10 electrons [2]. In the Malmberg-trap configuration employed for this experimental study, the typical axial length of the electron plasma is L = 235 mm over the cross section so that $n_e(x,y) = N_l(x,y)/L$ [3-5].

A new feature we have introduced to the arena of vortex dynamics researches is an array of small electron emitters each of which can be operated independently. Various configurations of electron strings (point vortices in 2D space) can be generated as the initial distribution or added sequentially [3-5]. Point vortices have played

*Corresponding author's e-mail: m52279@sakura.kudpc.kyoto-u.ac.jp

significant roles in researches of 2D turbulence both with dynamical approaches and with statistical approaches [6]. Different shapes and levels of continuous vorticity distribution can also be generated by combining repeated injection, relaxation and partial dumping of trapped electrons. [5].

In this paper we report some fundamental processes that is involved in the evolution of 2D turbulence by starting with controlled initial conditions of vorticity distribution. Some other topics are presented in separate papers in this conference [7,8]

2, Discrete Vortices in Vacuum

The 2D location (x,y) of a point-like discrete vortex α interacting with other point-like vortices in the trap of radius R is described in the complex plane with $z = x + iy$ as,

$$\frac{dz_\alpha^*}{dt} = \frac{dw(z)}{dz}\Big|_{z_\alpha} - i\Omega\left(|z_\alpha|\right)z_\alpha^*, \qquad (1)$$

where

$$w(z) = \sum_{\beta\neq\alpha}\frac{\Gamma_\beta}{2\pi i}\ln\left(\frac{z}{z_\beta}-1\right) - \sum_\beta \frac{\Gamma_\beta}{2\pi i}\ln\left(\frac{z}{R}-\frac{R}{z_\beta^*}\right). \qquad (2)$$

Here the first term stands for direct interactions with other vortices, and the second term comes from image charges induced on the conducting cylindrical wall at $|z| = R$ which conforms to the outermost stream line $\psi(R)$. The circulation Γ_β of vortex β is related to the electron density as follows:

$$\Gamma_\beta = \iint_{S_\beta} dx'dy'\zeta(x',y') = \iint_{S_\beta} dx'dy'\frac{en_e(x',y')}{\varepsilon_0 B_0} \approx \frac{eN_\beta}{\varepsilon_0 B_0 L}. \qquad (3)$$

Here S_β is the cross-section of the vortex patch β consisting of N_β electrons. The frequency $\Omega(|z|)$ represents the external drive that is generated from the radial electric field associated with the end-plugging potential.

Experimental confirmation of the Hamiltonian dynamics as represented by Eq. (1) has been carried out for small number of point vortices [3,4]. Increasing the initial number of vortices introduces stochasticity in the evolution of the point vortex dynamics, and leads to punctuated merging among discrete vortices [9].

One example is shown in Fig. 1. Here the initial distribution of 19 vortices goes into a random state of motion until it reaches a meta-equilibrium state of 8 vortices. Before all the vortices merge into the single-

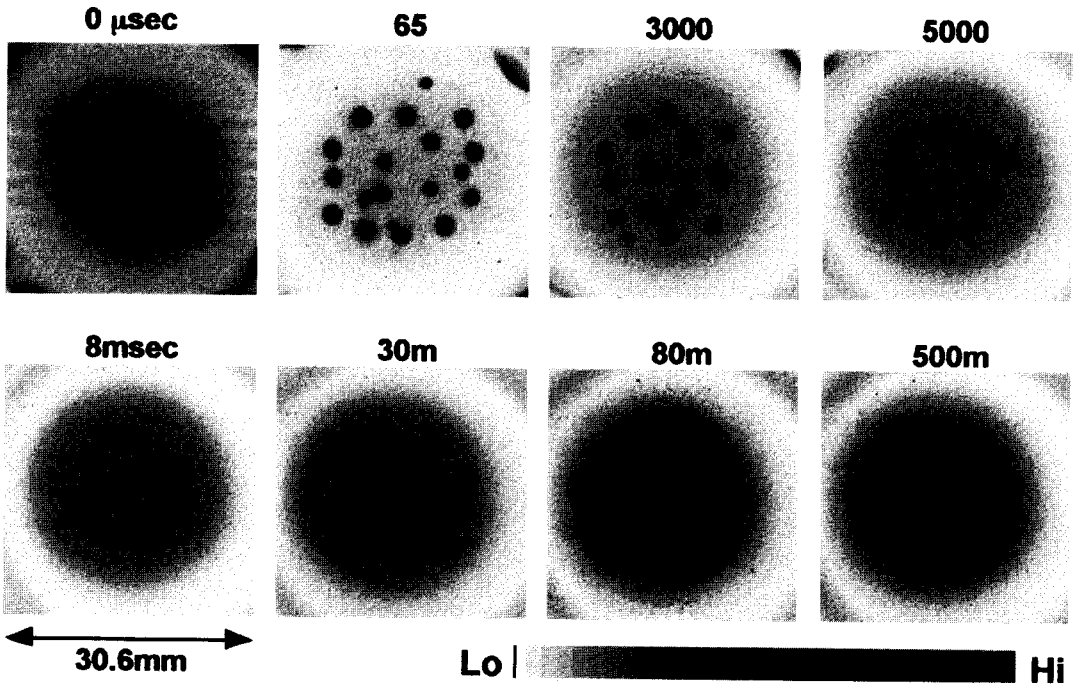

Fig. 1 Evolution of interacting discrete-vortex system to ordered states.

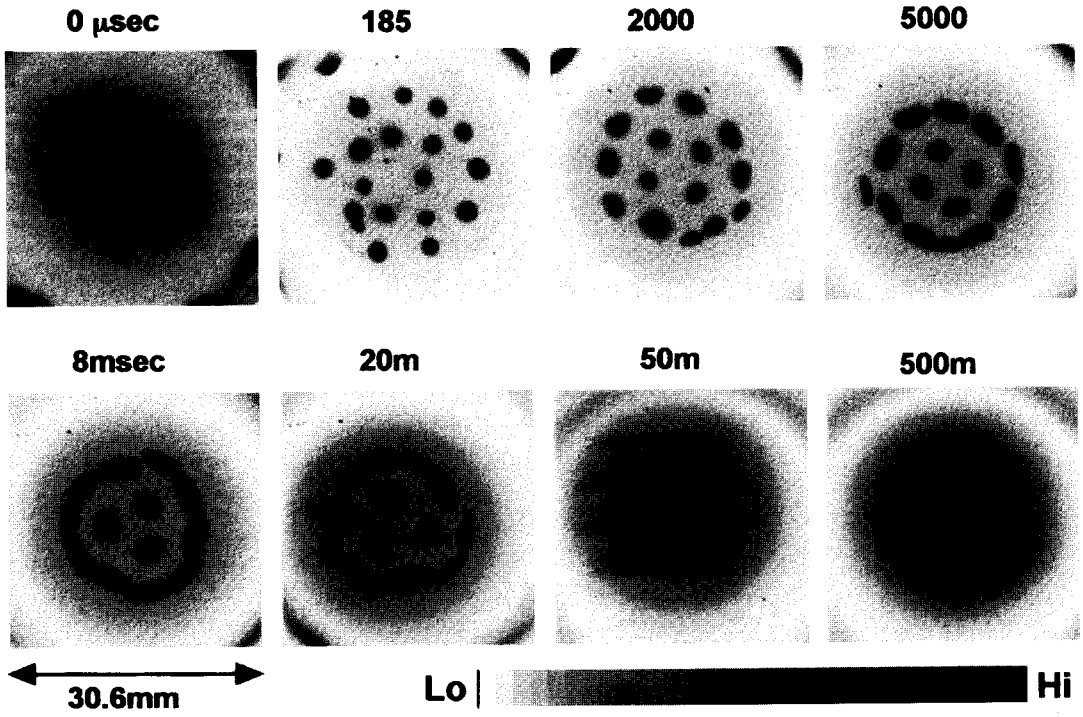

Fig. 2 Evolution of interacting discrete-vortex system to ordered states. The radial potential profile at the ends is slightly flattened.

vortex state, there appear several stages of meta-equilibrium configurations. Such crystal-like states have already been observed to evolve from random distributions of vortices created by Kelvin-Helmhortz instability under the magnetic field stronger than our case by a factor more than 10 [9]. Mildness in the profile of each vortex is most probably attributed to the weakness of the present magnetic field $B_0 < 0.048$ T.

Figure 2 shows another observation that slight flattening of the radial profile of the vacuum potential at the plugging zone leads to different configurations of the vortex crystal that has inner ring consisting of 4 or 3 (later) vortices. The difference in Fig. 2 may be attributed to a reduction of the radially-increasing azimuthal-drive due to the radial electric field of the confining potential. This vacuum-field drive tends to compensate the rotational shear driven by the self-field of the electron vortices.

In the process of the relaxation relatively weak strings are broken into thin sheets, and get folded into a stronger vortex coming nearby. A noticeable process involved here is that some fraction of the sheet remains unabsorbed and forms a rugged background vorticity distribution. The self-generated background vortices appear significantly to affect the process of interactions among remaining vortex patches.

3. Single Vortex Dynamics in Background Vortex

As an important elementary process we examine the dynamics of a single vortex in interaction with a background vorticity distribution [3-5]. In the short history of our experimental studies this type of interaction came out as a basic problem that is simplified from the two-vortex interaction as discussed later. This configuration is among well-discussed processes in planetary atmosphere, and qualitative behavior has been examined experimentally with normal fluids. Quantitative examination became available only after Schecter and Dubin proposed a theoretical model based on linearized Euler fluid equation of motion [10]. The radial velocity of a point vortex projected to the gradient of the background distribution is given in terms of differential equation,

$$\frac{dr}{dt} = \frac{\Gamma_v}{2\pi} \frac{d\zeta_b / dr}{|A|} \ln\left(\frac{cr}{l}\right) \arctan\left(\frac{|A|t}{2}\right), \qquad (4)$$

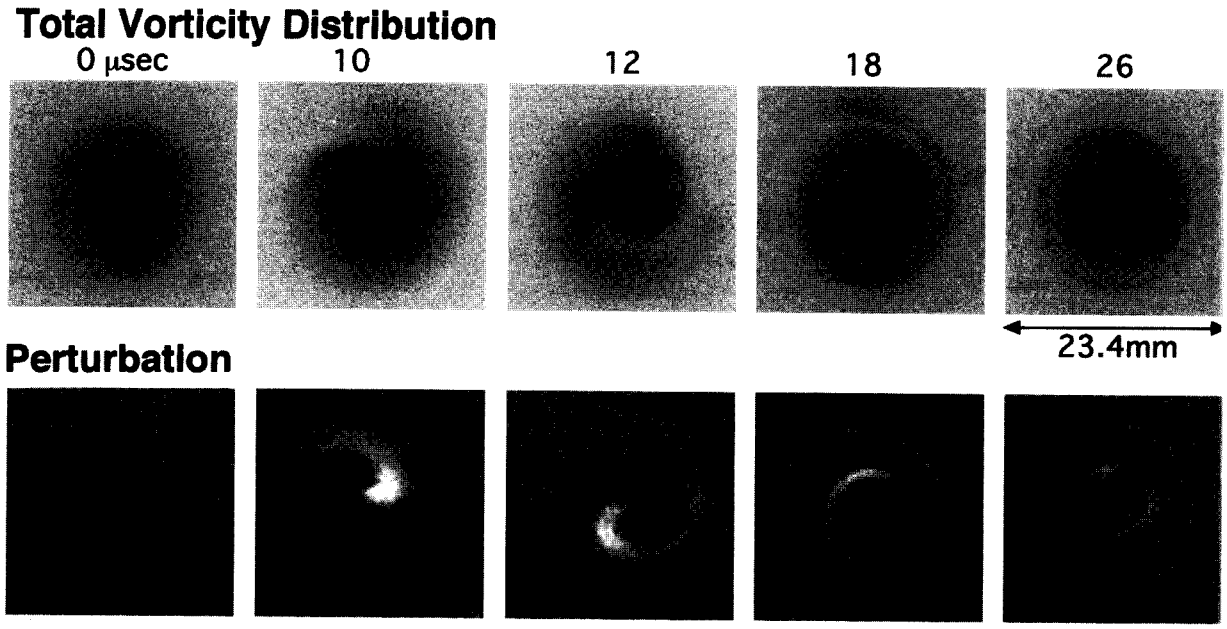

Fig. 3 Motion of a single point vortex in the background vorticity distribution. From Ref. 5.

where $A = -rd\Omega_b(r)/dr$ is the shear relative to the local rigid rotation

$$\Omega_b(r) = \frac{e}{\varepsilon_0 B_0 r^2} \int_0^r drrn_b(r)$$

of the background vortex, $l = (\Gamma_v/2\pi|A|)^{1/2}$ is the radius of the stagnation zone around the point vortex with a circulation of Γ_v, and c is a number of order 1.

In short this model predicts that a point-like vortex moves up along the gradient of the background vorticity with an extended distribution. The direction of the motion of the point vortex has been confirmed for different shapes of the background vortex including convex and concave (unstable) radial distributions [5]. Though the fluid dynamical expression appears highly mathematical, it turned out much easier to understand if we interpret this process in terms of plasma physics [5].

Figure 3 displays snapshots of the vorticity distribution after a single vortex string is placed at the periphery of a background vortex with a radial distribution that decreases monotonically. The upper panel shows the total distribution, and the lower panel shows the perturbation in the background distribution [5]. The point vortex moves radially up the hill of the background while orbiting azimuthally around it under the drive of the $\boldsymbol{E} \times \boldsymbol{B}$ drift. A spiral streak of the vorticity perturbation is generated behind the point vortex and remains long after it reaches the center of the background. The level of the perturbation increases with the strength ($\propto N_v$) of the point vortex. Observations indicate that on the arrival of the point vortex the local perturbation level goes up to several tens of percent and stay at this level even after the vortex moves away.

Figure 4 shows the time evolution of the radial distance of apoint vortex from the center of the background vortex for different strengths of $\Gamma_v \propto N_v$, where $N_v/10^6$ = 1.6 (△), 4.4 (□), 8.7 (○), 17 (●) [5]. The electron string is electrically disconnected from the cathode at the time t = 15 μs as indicated by the arrow. The inset shows the common profile of the initial background in unit of 10^{13} m^{-3} with $N_b = 7.8 \times 10^7$. The arrow here indicates the initial position of the point vortices. The curves attached to the dots denote the orbits as calculated from eq. (4) by using experimentally determined parameters. Well before the point vortex reaches the background center, the observed radial orbits agree with the theoretical expectation as given by solidcurves.

The characteristic time, required for the point vortex to travel between 10 % and 90 % positions along the initial path of the radial distance from the background center, is evaluated from the experimental data as shown in Fig. 4, and plotted in Fig. 5 as a function of τ_{Model}. The the oretically expected time τ_{Model} is evaluated from eq. (4) by introducing the experimental parameters including the initial profile of

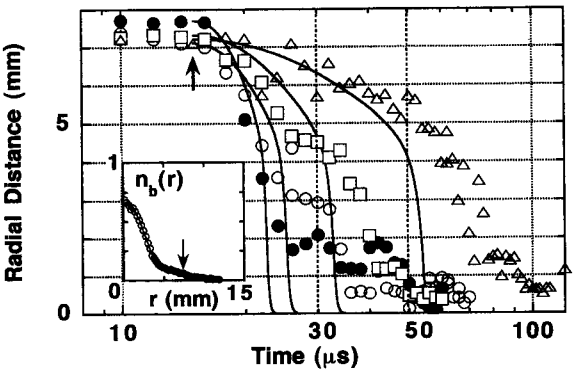

Fig. 4 Radial distance of a single point vortex from the background vortex center.

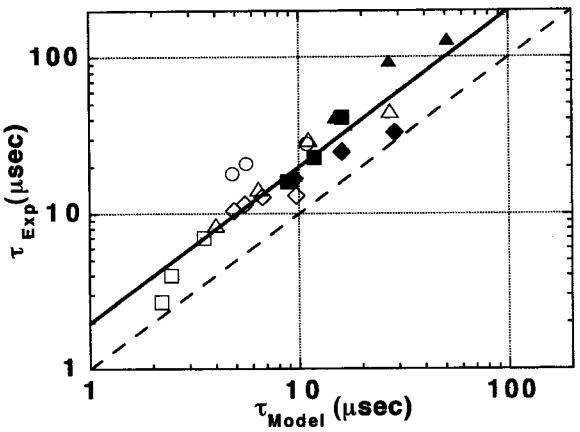

Fig. 5 The observed time (in the ordinate) for the point vortex to climb the background vorticity hill is compared with the theoretical prediction (in the abscissa). From Ref. 5.

the background distribution and N_v. It is found that the experimental values of τ_{Exp} are nearly the twice of τ_{Model} [5]. The difference in the constant factor is attributed to merely replacing the logarithmic factor in Eq. (4) to 1 to avoid a mathematical singularity coming from the simplification of the model.

The spiral structure observed in Fig. 3 rotates differentially with respect to the point vortex. It can produce time-varying electric field that may affect the motion of the point vortex. Oscillations have been actually observed in the time history of the vortex distance from the background center as shown in Fig. 4 [5]. The oscillations are not expected from the theoretical model.

From electron density distributions that are obtained with improved sensitivity and resolution of imaging diagnostics, we have constructed 2D distributions of the potential and electric field [2]. It is shown that the spiral structures in the vorticity distribution actually generate azimuthal electric field at the position of the point vortex and can drive it radially in and out at the velocity consistent with that evaluated from Fig. 4 [7].

The discussion in this section indicates that the distribution of background vortex is modified substantially by a discrete vortex with high local density and the modified distribution exerts influences back to the latter.

4. Two Vortex Interaction in Background Vortex

As an elementary process in the interaction among discrete vortices, we examine trajectories of two discrete vortices immersed in different levels of background vorticity. Example frames of the vorticity distribution are shown in Fig. 6. In contrast to the dynamics in vacuum, the two vortices approach in a time shorter by orders of magnitude either to merge into one or to form a binary vortices. The binaries revolve stably at a distance of less than two vortex diameters at which they should get merged in vacuum [11].

As depicted in Fig. 7 that was obtained in the preliminary stage of our study [4], the time τ required for the two vortices approach decreases almost proportionally to the inverse of the total circulation $\Gamma_b \propto N_b$ of the background. At the time of this experiment our diagnostic system was not sensitive enough to determine the profile of the background vorticity. After the proposal of the theoretical model [10], we made a rough evaluation of the time scale by assuming that each of the discrete vortices climbs the background hill independently until they come close within the distance of their diameter [4]. The naive evaluation gives a right order of the time scale, but reasonable scaling cannot be obtained in regard to the parameter dependence.

The difference in the applicability of the theoretical model to the single-vortex and two-vortex cases has lead us to consider that the background vorticity distribution is significantly modified by the discrete vortices and that it gives substantial influence back to the vortices. Figure 6 shows an example taken from recent data that came available after a substantial improvement of the diagnostics. It reveals that intricate structures appear in the background distribution especially in the case where the binary vortices are formed.

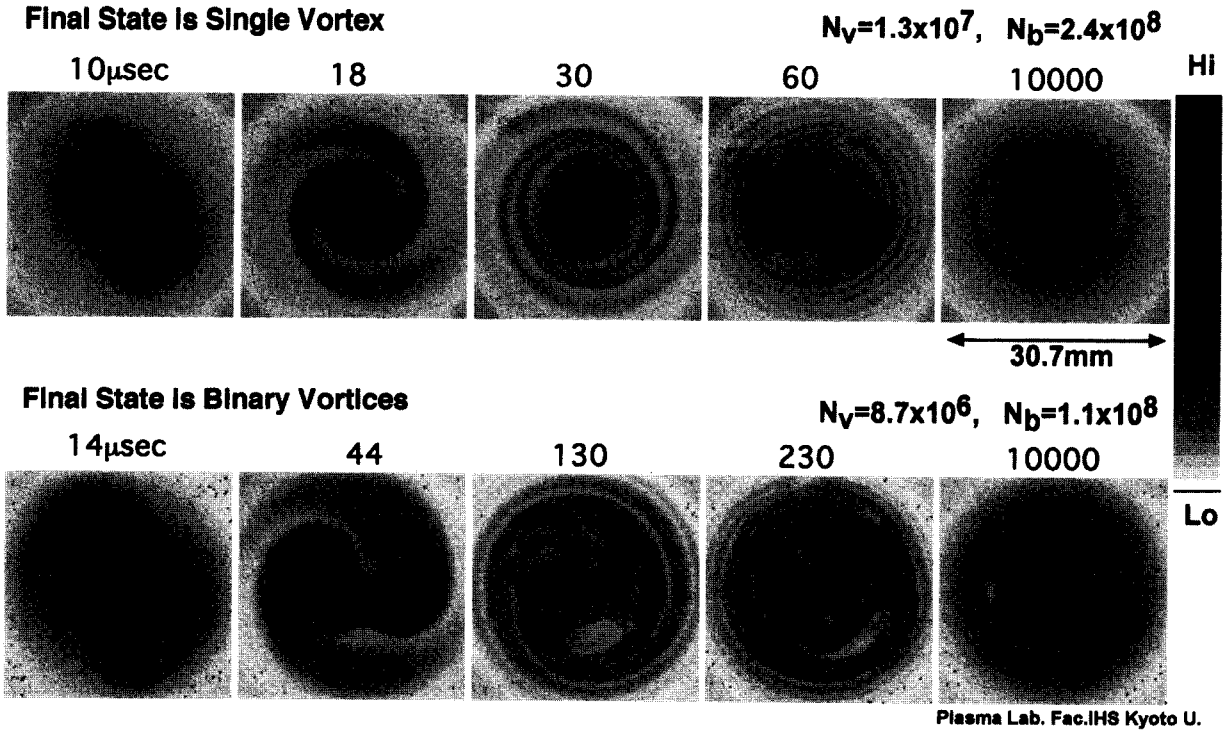

Fig. 6 Interacting two discrete vortices in a background vortex.

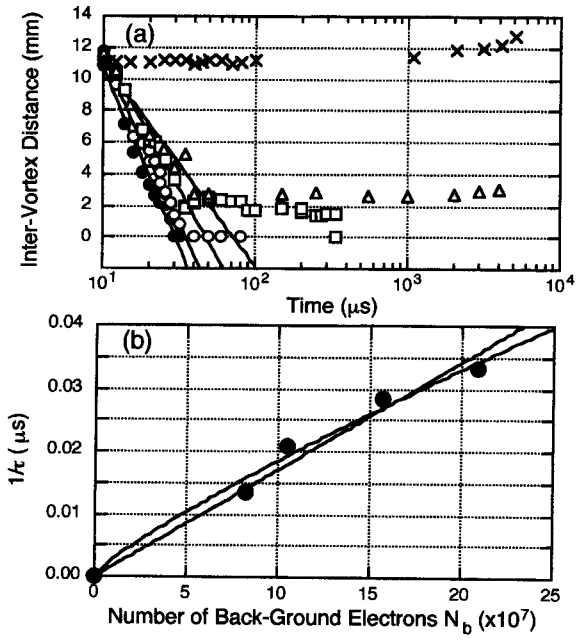

Fig. 7 (a) Two discrete vortices approaches faster as the circulation of the background vortex $\Gamma_b \propto N_b$ increases. $N_b/10^8$ = 0 (×), 0.83 (△), 1.0 (□), 1.6 (○), 2.2 (●). (b) Merging time τ scales as $\propto N_b^k$ with k = 0.83 – 1. From Ref. 4.

5. Holes and Humps in Background Vorticity Distribution

Isolated depressions (holes) in the vorticity distribution have been invoked as a controlling factor in the evolution of 2D turbulence [10,12]. Such holes have been observed in our experiments. But, in many cases, we also have observed rings of dip or rings of hump of the vorticity around unmerged discrete vortices. Holes around discrete vortices have been invoked as a transport barrier of entropy in the statistical approach to the formation of the vortex crystal [13]. Our observation shows that the circulation of the ring hole (decrement from the background) is 5 to 20 % of the clump in the core. Though the field of a discrete vortex may not be fully shielded, the ring-shaped holes or sometimes ring-shaped humps appear to weaken the direct interaction between the discrete vortices and to keep them away from merging.

Our current understanding is that such contribution of the background vorticity should be essential to accelerating the process of organizing meta-equilibrium structures and also effective to slow down the process of disintegration until some imbalance grows so that reorganization proceeds in a punctuated manner.

Detailed examinations about the generation mechanism and properties of the ring holes are reported in a separate paper [8].

6. Conclusions

We have examined fundamental processes in the evolution of 2D turbulence under precise control of the initial vorticity distribution. The plasma-physical approach is demonstrated to be effective in elucidating intricate physical mechanisms that largely remain behind the mathematical expressions of fluid dynamics,

Acknowledgments

The authors thank Prof. A. Mohri for stimulating discussion. This work was supported by a Grant-in-Aid from the Ministry of Education, Science, Sports and Culture and partly by the collaborative research program of National Institute for Fusion Science.

References

[1] R.H. Levy, Phys. Fluids **11**, 920 (1968).

[2] K. Ito, Y. Kiwamoto and A. Sanpei, Jpn. J. Appl. Phys. **40**, 2558 (2001).

[3] Y. Kiwamoto, A. Mohri, K. Ito, A. Sanpei and T. Yuyama, *Non-neutral Plasma Physics* III (AIP1999) pp.99-105.

[4] Y. Kiwamoto, K. Ito, A. Sanpei, A. Mohri, T. Yuyama and T. Michishita, J. Phys. Soc. Jpn. (Lett.) **68**, 3766 (1999).

[5] Y. Kiwamoto, K. Ito, A. Sanpei and A. Mohri, Phys. Rev. Lett. **85**, 3173 (2000).

[6] *See, for example*, J. Miller, P.B. Weichman and M. C. Cross, Phys. Rev. A **45**, 2328 (1992).

[7] K. Ito, Y. Kiwamoto and A. Sanpei, *poster PII-52 in this conference.*

[8] A. Sanpei, Y. Kiwamoto and K. Ito, *poster PII-51 in this conference.*

[9] K.S. Fine, A.C. Cass, W.G. Flynn and C.F. Driscoll, Phys. Rev. Lett. **75**, 3277 (1995).

[10] D.A. Schecter and D.H.E. Dubin, Phys. Rev. Lett. **83**, 2191 (1999).

[11] T.B. Mitchell, C.F. Driscoll and K.S. Fine, Phys. Rev. Lett. **71**, 1371 (1993).

[12] X.-P. Huang, K.S. Fine and C.F. Driscoll, Phys. Rev. Lett. **74**, 4424 (1995).

[13] D.Z. Jin and D.H.E. Dubin, Phys. Rev. Lett. **80**, 4434 (1998).

[14] A.A. Kabantsev, C.F. Driscoll, D.H.E. Dubin and D.A. Schecter, *invited paper in this meeting.*